Preferred Gimbal Angles for Single Gimbal Control Moment Gyros

S. R. Vadali,* H.-S. Oh,† and S. R. Walker‡
Texas A&M University, College Station, Texas 77843

This paper deals with torque command generation using single gimbal control moment gyros. The angular momentum and torque envelopes are assumed to be known a priori. A method based on back integration of the gyro torque equation from desired final conditions is used to determine a family of initial gimbal angles that avoid singularities. Each member of this family is defined as a preferred initial gimbal angle set. The pseudoinverse steering law is used during the numerical integrations. This procedure is demonstrated by means of numerical examples that include attitude control and momentum management of the Space Station Freedom. A feedback control scheme based on "null motion" is also developed to position the gimbals at preferred angles.

Introduction

CONTROL moment gyros (CMGs) are attractive spacecraft attitude-control devices. They require no expendable propellant, which is a limited resource and can contaminate the spacecraft environment. Their fixed rotor speeds minimize structural dynamic excitations. They can be used for rapid slewing maneuvers and precision pointing. For low Earth orbiting spacecraft, momentum dumping can be easily achieved by gravity-gradient torques. From the steering-law viewpoint, it is widely accepted that double-gimbal CMGs (DCMGs) are preferable to single-gimbal CMGs (SCMGs). For DCMGs, steering laws proposed by Kennel[1,2] have been well accepted. The SCMGs have the advantages of possessing relative mechanical simplicity and producing amplified torques (for low spacecraft angular velocities) on the spacecraft. However, development of gimbal steering laws for their use is made difficult by the existence of internal singular states. For any system of n CMGs and any direction in space, there exist 2^n sets of gimbal angles[3] for which no torque can be produced in that direction, and these sets are called internal singularities. External singular states correspond to directional angular momentum saturation. DCMGs have internal singularities also, but they are easier to avoid.

Margulies and Aubrun[3] present a geometric theory of SCMG systems. They characterize the momentum envelope of a cluster of SCMGs and identify the internal singular states. Yoshikawa[4] presents a steering law for a roof-type configuration with four SCMGs. His steering law is based on making all of the internal singular states unstable by providing two jumps with hystereses around the singularities. Cornick[5] develops singularity avoidance control laws for the pyramid configuration. His technique is based on the ability to calculate the instantaneous locations of all singularities. Hefner and McKenzie[6] develop a technique for maximizing the minimum torque capability of a cluster of SCMGs in the pyramid configuration. Bauer[7] concludes that it is impossible to avoid some singularities and, in general, no global singularity-avoidance steering law can exist. Consequently, there will be instances when torque demand cannot be met exactly.

Received May 22, 1989; presented as Paper 89-3477 at the AIAA Guidance, Navigation, and Control Conference, Boston, MA, Aug. 14–16, 1989; revision received Oct. 17, 1989.

*Assistant Professor of Aerospace Engineering. Member AIAA.
†Graduate Student. Student Member AIAA.
‡Graduate Student; currently Engineer, Rockwell Shuttle Operation, Houston, TX.

Meffe[8] presents a parametric tradeoff study between CMG systems (type and number) for the space station. Specifically, the indicators are reliability, weight, power, volume, maintenance, safety, control law, and life-cycle cost. The conclusions are in favor of either the 4/6 or 5/6 SCMG clusters. The numbers 4/6 indicate a total of six CMGs with four being active. The Soviet space station MIR uses the 4/6 SCMG cluster. The DCMG clusters are found superior to SCMG clusters only from power consumption viewpoint. In a recent paper, Blondin et al.[9] discuss the selection of a prototype DCMG for the space station. One of the reasons behind this choice is that the space station does not have requirements to perform rapid maneuvers.

The requirements for the space station are to control the attitude in the presence of disturbance torques due to environmental effects, motion of sun-tracking devices, and Shuttle docking. Besides the attitude constraints of torque equilibrium attitude (TEA) reference within 10 deg of local vertical local horizontal (LVLH) and rates less than 0.02 deg/s, the CMG momentum must be restricted[8] to a spherical storage radius (initial phase) of 20,000 ft-lb-s. The torque is limited to 400 ft-lb (spherical). These figures are subject to change. An active momentum management and attitude controller for the space station has been developed by Wie et al[10] and Warren et al.[11] This scheme seeks TEA and provides periodic-disturbance rejection. The design of the pitch-axis controller is decoupled from that of roll-yaw. Periodic-disturbance rejection filters are developed to reject disturbances in the attitude or angular momentum at the orbital rate and multiples of the orbital rate. CMG dynamics and steering laws have not been considered in this work.

In the present paper, we consider the determination of initial gimbal angles for SCMG systems to avoid internal singularities. Throughout the study, four SCMGs in a pyramid configuration shown in Fig. 1 are used. The motivation for this study came from earlier works mentioned previously, wherein it has been shown that many singularity-avoidance steering laws are not capable of avoiding singularities consistently even for unidirectional torque demands. We approach the torque-generation problem from a more conservative viewpoint. Rather than trying to develop a singularity-avoidance law, we present a simple procedure for determining the preferred initial gimbal angles for specific torque and momentum envelopes. In many instances, these can be obtained by performing attitude-control simulations without including the CMG dynamics for a variety of initial conditions, parameter variations, and so forth. The proposed method is based on back integration of the CMG torque equation, typically starting near the saturation envelope (to utilize the entire envelope)

and going to the specified initial angular momentum state. The pseudoinverse steering law is used during the numerical integration. It is shown by means of examples given in the literature that the preferred initial gimbal angles do avoid internal singularities. Finally, the attitude control and momentum management of the phase I space station is considered as an additional example. This example clearly shows the advantage of using a preferred set of initial gimbal angles.

An important issue is the reorientation of the gimbals from arbitrary angles to a preferred set. A feedback scheme for performing such reorientations while minimizing output torques on the spacecraft is also discussed.

CMG Steering

We consider CMG gimbal steering for four SCMGs mounted in the pyramid configuration shown in Fig. 1. It is assumed that the x,y,z axes (roll, pitch, and yaw, respectively) shown in the figure coincide with the vehicle body axes, and the center of the pyramid base is assumed to be located at the center of mass of the vehicle. Only the axial angular momentum of each CMG is included in the mathematical model. The angular momentum vector $\boldsymbol{h}$ and its derivative $\dot{\boldsymbol{h}}$ in the body axes can be written as

$$\dot{\boldsymbol{h}} = h \begin{Bmatrix} -\cos\delta \sin\sigma_1 - \cos\sigma_2 + \cos\delta \sin\sigma_3 + \cos\sigma_4 \\ \cos\sigma_1 - \cos\delta \sin\sigma_2 - \cos\sigma_3 + \cos\delta \sin\sigma_4 \\ \sin\delta \sin\sigma_1 + \sin\delta \sin\sigma_2 + \sin\delta \sin\sigma_3 + \sin\delta \sin\sigma_4 \end{Bmatrix} \quad (1)$$

and

$$\dot{\boldsymbol{h}} \triangleq C\dot{\sigma} = h \begin{bmatrix} -\cos\delta \cos\sigma_1 & \sin\sigma_2 & \cos\delta \cos\sigma_3 & -\sin\sigma_4 \\ -\sin\sigma_1 & -\cos\delta \cos\sigma_2 & \sin\sigma_3 & \cos\delta \cos\sigma_4 \\ \sin\delta \cos\sigma_1 & \sin\delta \cos\sigma_2 & \sin\delta \cos\sigma_3 & \sin\delta \cos\sigma_4 \end{bmatrix} \begin{pmatrix} \dot{\sigma}_1 \\ \dot{\sigma}_2 \\ \dot{\sigma}_3 \\ \dot{\sigma}_4 \end{pmatrix} \quad (2)$$

where h is the constant magnitude of the axial angular momentum of each CMG, σ_i the gimbal angles, and δ the pyramid angle as shown in Fig. 1.

The Euler equations for a system consisting of a spacecraft and a CMG cluster can be written as

$$[I]\,\dot{\omega} + \dot{\boldsymbol{h}} + \omega \times \{[I]\,\omega + \boldsymbol{h}\} = 0 \quad (3)$$

where $[I]$ is the inertia matrix of the spacecraft and ω is the angular velocity vector; $\omega\times$ indicates the cross product operation. We can write Eq. (3) as

$$[I]\,\dot{\omega} + \omega \times [I]\omega = -\dot{\boldsymbol{h}} - \omega \times \boldsymbol{h} \triangleq -\boldsymbol{u} \quad (4)$$

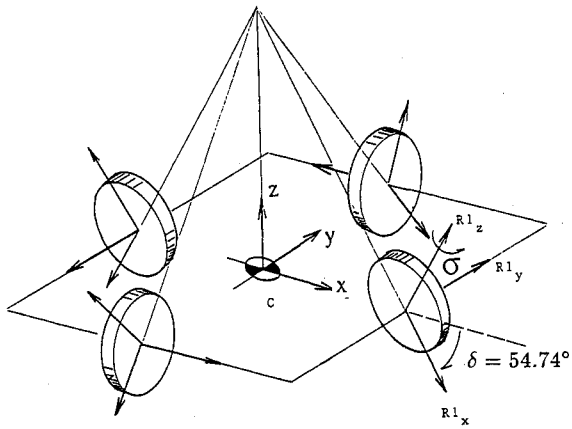

Fig. 1 Pyramid configuration.

where $\boldsymbol{u}$ is the internal torque vector. The CMG steering equation is written, using Eqs. (2) and (4), as

$$C\dot{\sigma} = \boldsymbol{T} \quad (5)$$

where

$$\boldsymbol{T} \triangleq -\omega \times \boldsymbol{h} + \boldsymbol{u} \quad (6)$$

The usual procedure for obtaining the gimbal rates from Eq. (5) is to use the pseudoinverse of C. Thus we have

$$\dot{\sigma} = C^T (CC^T)^{-1} \boldsymbol{T} \quad (7)$$

The determinant of the matrix CC^T can be thought of as the average gain of the cluster. It is well known that if rank (CC^T) is less than three, the pseudoinverse does not exist. The sets of states at which this happens are called singular states or singularities. Many steering laws have been developed to avoid singular states, yet none has been proven to do so consistently. A factor common to these schemes is the addition of "null motion," —motion of the gimbals such that no torque is produced on the spacecraft. In many situations, it is difficult to anticipate the approaching singular states fast enough to add sufficient null motion. The scheme proposed by Kurokawa et al.[12] is based on off-line calculation and table look-up of gimbal angles that globally maximize the gain for a given momentum. This scheme also has not been able to provide singularity-free steering. As mentioned previously, our objective is to develop a systematic approach for determining a set of initial gimbal angles that can avoid singular states for a given torque and momentum envelopes. This is discussed in the next section.

Determination of Preferred Initial Gimbal Angles

Perhaps the most severe demand on the CMGs is a secular torque [$\boldsymbol{T}$ in Eq. (6)]. Bauer[7] shows that for the present CMG configuration ($\delta = 54.74$ deg), with the pseudoinverse steering law, starting with all of the gimbal angles at zero, for a constant positive torque about the x axis, an internal singularity is encountered at a momentum value of $1.15h$. This corresponds to an antiparallel situation, i.e., two of the CMG angular momentum vectors are pointed in opposite directions. The gimbal angles at the singularity are $\sigma = [-90$ deg, 0 deg, -90 deg, 0 deg $]^T$. The gimbal rates, without imposed constraints, are large near a singularity. It is noted that for the same torque demand, multiple gimbal angle trajectories can exist from one momentum state to another. A set of initial gimbal angles that allows smooth gimbal rates throughout, up to saturation, is termed "a preferred set." To investigate the existence of preferred sets, a backward integration of Eq. (7) was attempted, for specified torque demands.

At saturation along the positive x axis, all of the momentum vectors are maximally projected along the x axis, i.e., $\sigma = [-90$ deg, 180 deg, 90 deg, 0 deg$]^T$ and $\boldsymbol{h} = [h(2\cos\delta + 2), 0, 0]^T = [3.1545h, 0, 0]^T$. The saturation gimbal angles for a given direction are unique. Since saturation is an external singularity, we cannot start the integration process exactly there. Hence, the gimbal angles were perturbed slightly. For example, we selected the near-saturation angles as $\sigma = [-89$ deg,

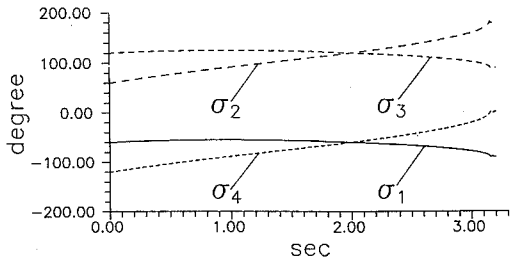

Fig. 2 Gimbal angles for unit x-axis torque $\sigma(0) = [-60$ deg, 60 deg, 120 deg, -120 deg$]^T$.

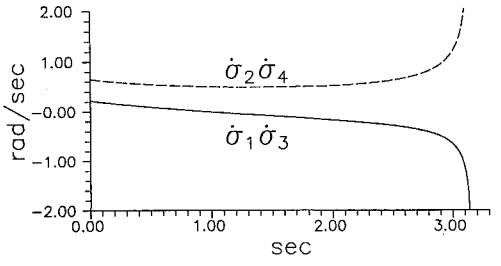

Fig. 3 Gimbal rates for unit x-axis torque $\sigma(0) = [-60$ deg, 60 deg, 120 deg, -120 deg$]^T$.

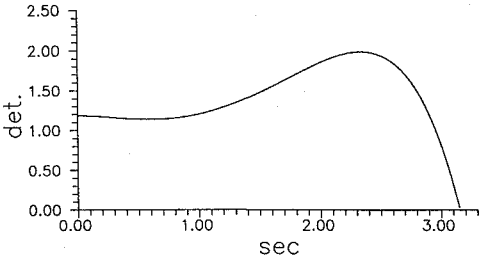

Fig. 4 Gain for unit x-axis torque.

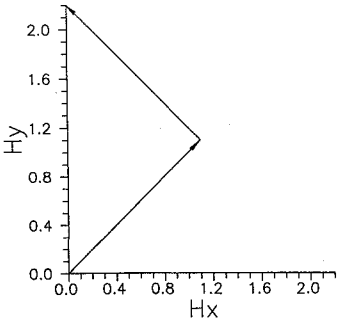

Fig. 5 Angular-momentum requirement for Bedrossian example.

Table 1 Initial gimbal angles for null momentum

Torque demand	Initial gimbal angles	
[1 0 0]	[− 60 deg 60 deg 120 deg −120 deg]	[45 deg −45 deg 45 deg −45 deg]
[0 1 0]	[−120 deg −60 deg 60 deg 120 deg]	[45 deg −45 deg 45 deg −45 deg]
[0 0 1]	[0 deg 0 deg 0 deg 0 deg]	
[1 1 1]	[0 deg 0 deg 0 deg 0 deg]	[45 deg −45 deg 45 deg −45 deg]
[4 2 0]	[− 60 deg 60 deg 120 deg −120 deg]	[45 deg −45 deg 45 deg −45 deg]
[2 4 0]	[−120 deg −60 deg 60 deg 120 deg]	[45 deg −45 deg 45 deg −45 deg]

177 deg, 90 deg, -1 deg$]^T$. This choice is arbitrary and forces the selection of one of the many trajectories leading toward the zero-momentum state. On back integration of Eq. (7), with a unit torque along the x axis, the following gimbal angles were obtained near the zero-angular momentum state: [-59.6 deg, 60.7 deg, 118 deg, -121 deg$]^T$. The angular momentum vector at this point was [0.003, -0.023, 0.029$]^T$. It is interesting to note that singularities were not encountered during this process. The nearest gimbal angles for the zero-angular-momentum state are $\sigma = [-60$ deg, 60 deg, 120 deg, -120 deg$]^T$. These initial gimbal angles provide a local maximum for the CMG gain for zero momentum, which is 1.1854. The gimbal angles and rates with these preferred settings (forward integration with pseudoinverse steering law) are shown in Figs. 2 and 3. Figure 4 shows the CMG gain and it is clear that the gain margin is quite high throughout except near saturation. Moreover, near the x axis momentum of 1.15, the gain is increasing. It can be verified that a pseudoinverse steering law with this initial gimbal angle set does indeed avoid all singular states for torques along the x axis.

Several sets of initial gimbal angles for null momentum were obtained for other desired torques as shown in Table 1. It should be noted that due to symmetry of the configuration, the set [-120 deg, -60 deg, 60 deg, 120 deg] is admissible for a torque demand of [0 1 0$]^T$.

Preferred gimbal angles for nonzero momentum states can also be obtained by this procedure. It is also interesting that the set [45 deg, -45 deg, 45 deg, -45 deg] provided singularity-free operation for all of the examples in Table 1, except for the uniaxial z-torque example.

Kurokawa et al.[12] consider the following torque demand:

$$T_x = 0.2 \sin(4\pi t)$$

$$T_y = 0.3$$

$$T_z = 0.0$$

Our simulations were performed with gimbal angles initially set at [-120 deg, -60 deg, 60 deg, 120 deg] as well as [45 deg, -45 deg, 45 deg, -45 deg]. These choices were made because the torque lies in the x-y plane. No internal singular gimbal states were encountered and saturation occurred at about 10 s.

The next example is similar to that considered by Bedrossian.[13] The required angular momentum distribution is shown in Fig. 5. The absolute values of the x and y components of the torque are held constant at 0.707. Gimbal rates with zero initial angles are shown in Fig. 6. It is clear that a singularity is encountered at 1.5 s. Figure 7 shows the gimbal rates with the preferred set [45 deg, -45 deg, 45 deg, -45 deg] . It is evident that no singularities are encountered. Figure 8 shows the gain along the trajectory and again we see that there is sufficient gain margin and the gain is increasing near the region where a singularity was encountered during the previous simulation (Fig. 6).

Space Station Example

We now consider the attitude control and momentum management of the space station. This study also includes input

disturbances that are not used in the control design model. The space station data are given in Table 2. Although the angular momentum storage capability of 20,000 ft-lb-s dictates the use of 5/6 CMGs, we only use four. The following assumptions are made to obtain linearized equations: 1) Products of inertia are neglected; 2) the θ_1, θ_2, and θ_3 are small excursions from LVLH: roll, pitch, and yaw, respectively; and 3) the effect of CMG gimbal and rotor transverse inertia is neglected.

The linearized equations are

$$I_1\dot{\omega}_1 + n(I_2 - I_3)\omega + 3n^2(I_2 - I_3)\theta_1 = -u_1 + w_1 \quad (8a)$$

$$I_2\ddot{\theta}_2 + 3n^2(I_1 - I_3)\theta_2 = -u_2 + w_2 \quad (8b)$$

$$I_3\dot{\omega}_3 - n(I_2 - I_1)\omega_1 = -u_3 + w_3 \quad (8c)$$

$$\dot{\theta}_1 - n\theta_3 = \omega_1 \quad (9a)$$

$$\dot{\theta}_3 + n\theta_1 = \omega_3 \quad (9b)$$

$$\dot{h}_1 - nh_3 = u_1 \quad (10a)$$

$$\dot{h}_1 = u_2 \quad (10b)$$

$$\dot{h}_3 + nh_1 = u_3 \quad (10c)$$

where I_1, I_2, and I_3 are moments of inertia, ω is the angular velocity vector of the space station, n is the orbital rate, h is the CMG angular momentum vector along the body axes of the space station, u is the torque vector, and w the vector of disturbance torques.

The design disturbance model[10] is

$$w_1 = 1 + \sin(nt) + 0.5\sin(2nt), \text{ ft-lb} \quad (11a)$$

$$w_2 = 4 + 2\sin(nt) + 0.5\sin(2nt), \text{ ft-lb} \quad (11b)$$

$$w_3 = 1 + \sin(nt) + 0.5\sin(2nt), \text{ ft-lb} \quad (11c)$$

One filter for each frequency of the model disturbance is used in each channel. The filter equations for pitch-attitude disturbance rejection are of the form[10]

$$\ddot{\alpha} + n^2\alpha = \theta \quad (12a)$$

$$\ddot{\beta} + (2n)^2\beta = \theta \quad (12b)$$

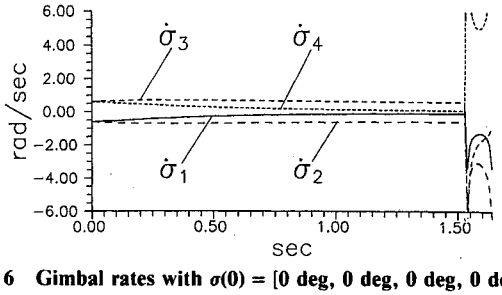

Fig. 6 Gimbal rates with $\sigma(0) = [0 \text{ deg}, 0 \text{ deg}, 0 \text{ deg}, 0 \text{ deg}]^T$.

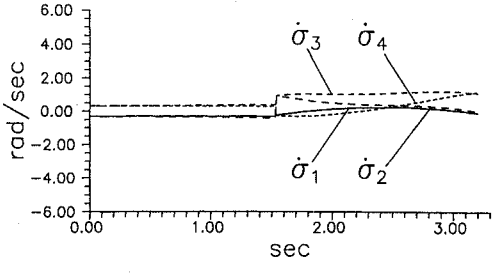

Fig. 7 Gimbal rates with $\sigma(0) = [45 \text{ deg}, -45 \text{ deg}, 45 \text{ deg}, -45 \text{ deg}]^T$.

A more refined disturbance model (AERO1 disturbance)[14] that includes variable aerodynamic drag characteristics is also included. The AERO1 disturbances are shown in Fig. 9. This model includes disturbances at higher frequencies than twice the orbit rate as well as orbit decay effects. In principle, one can filter out disturbances at three and four times the orbit rate using filters previously defined[11]; we have chosen not to do this, as our main aim is to assess CMG steering performance.

The pitch-axis controller is designed using LQR techniques.[10] The states are

$$x = [\theta_2, \dot{\theta}_2, h_2, \int h_2\, dt, \text{ and filter states}]$$

The states for the roll-yaw controller are

$$x = [\theta_1, \omega_1, h_1, \int h_1\, dt, \theta_3, \omega_3, h_3, \int h_3\, dt, \text{ and filter states}]$$

The state weighting matrix Q is selected to be diagonal and each entry is chosen such that $x_i\, Q_{ii}\, x_i = 1$, where x_i is the anticipated maximum value of the ith state. The control weighting matrix is selected to be the unity matrix. For the purpose of simulation, the initial attitude errors are selected to be 1 deg about each axis.

As h and u are known approximately after the controller design simulation, $\dot{h}$ can be thought of as a known quantity to determine steering histories for the gimbals. In flight operation, the CMG loop will be driven in parallel with the attitude-control loop. In the present context, the two loops have been separated for ease of simulation. This can be justified as the attitude-control bandwidth is low, of the order of 0.01 rad/s. For convenience, Eq. (5) is written as

$$C\dot{\sigma} = T$$

Table 2 Space station data

Quantity	Magnitude	Units
I_1	50.28E6	slug-ft^2 (roll)
I_2	10.80E6	slug-ft^2 (pitch)
I_3	58.57E6	slug-ft^2 (yaw)
n	0.0011	rad/s
h	3500	ft-lb-s

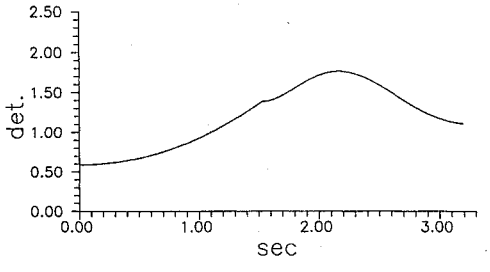

Fig. 8 Gain with $\sigma(0) = [45 \text{ deg}, -45 \text{ deg}, 45 \text{ deg}, -45 \text{ deg}]^T$.

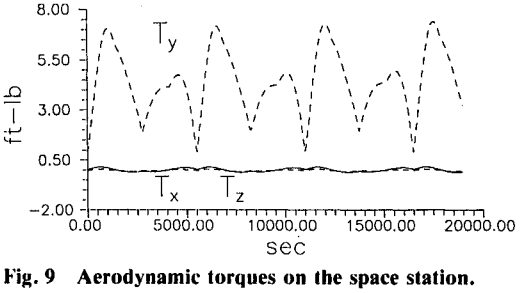

Fig. 9 Aerodynamic torques on the space station.

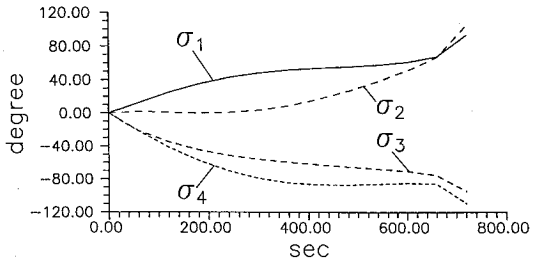

Fig. 10 Gimbal angles with $\sigma(0)$ = [0 deg, 0 deg, 0 deg, 0 deg]^T.

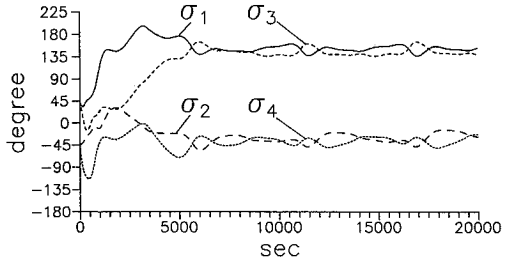

Fig. 11 Gimbal angles with $\sigma(0)$ = [45 deg, − 45 deg, 45 deg, − 45 deg]^T.

where

$$T = \begin{Bmatrix} u_1 + nh_3 \\ u_2 \\ u_3 - nh_1 \end{Bmatrix}$$

Starting with initial conditions of $\sigma = [0, 0, 0, 0]^T$, simulation of the pseudoinverse steering law shows that a singularity is encountered quite early in the first orbit (in about 720 s), as shown in Fig. 10.

From initial simulations without including CMG dynamics, we see that during the initial phases (less than one orbit) the pitch and roll momenta are much higher than the yaw momentum. Figure 11 shows the gimbal-angle histories with the initial gimbal angles selected as σ = [45 deg, − 45 deg, 45 deg, − 45 deg]^T. No singular states are encountered and the momentum magnitudes show near-periodic variations within limits. A small secular component is noticeable in the pitch aerodynamic torque due to orbit decay. This will lead to saturation of the CMGs if uncompensated for.

Gimbal Reorientation Using Null Motion

CMG momentum vectors can be repositioned at desired orientations by a feedback scheme using null motion. Let σ_f be the desired gimbal-angle set and σ the current gimbal-angle set. The relative error between the two is $e = \sigma_f - \sigma$. We define a candidate Lyapunov function

$$V = \tfrac{1}{2} e^T e$$

The time derivative of V can be written as

$$\dot{V} = e^T \dot{e} = -(\sigma_f - \sigma)^T \dot{\sigma} \tag{13}$$

If the reorientation process is to be performed without producing torques on the spacecraft, null motion equation for $\dot{\sigma}$ must be used. That is, let

$$\dot{\sigma} = [I - C^T(CC^T)^{-1}C]d \tag{14}$$

where d is any nonzero vector and I, the identity matrix.

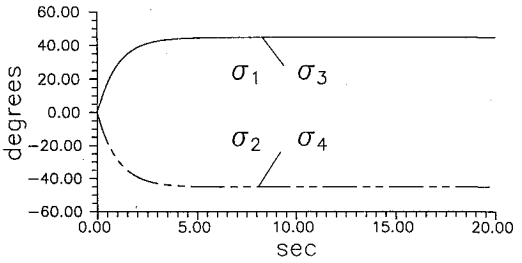

Fig. 12 Gimbal angles during reorientation.

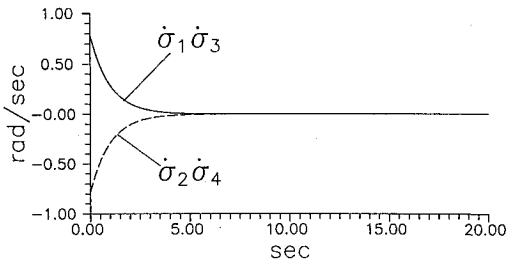

Fig. 13 Gimbal rates during reorientation.

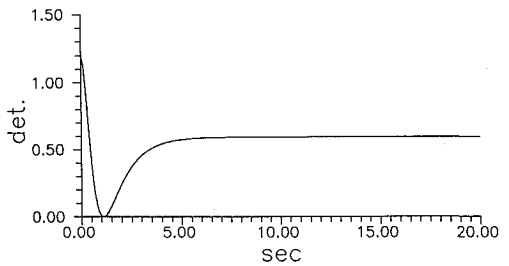

Fig. 14 Determinant (CC^T) during reorientation.

Equation (14) can be written as

$$\dot{\sigma} = \tau d \tag{15}$$

where $\tau = [I - C^T(CC^T)^{-1}C]$. It is easy to verify that if we premultiply Eq. (14) by C, the result is $C\dot{\sigma} = 0$. It is also important to note that $\tau^2 = \tau$, i.e., τ is a projection matrix. From Eqs. (13) and (15), it is clear that $\dot{V}$ is at least locally negative if

$$d = k(\sigma_f - \sigma) \tag{16}$$

where k is a scalar and

$$\dot{V} = -k(\sigma_f - \sigma)^T \tau (\sigma_f - \sigma) \tag{17}$$

Even though this scheme seems simple, there exists one drawback. If an internal singularity is encountered during the transit, τ becomes undefined. To avoid this problem, near a singularity, the following modification is made by using the so-called singular robustness inverse[13,15]:

$$\dot{\sigma} = [I - C^T(CC^T + \alpha I)^{-1} C]d \tag{18}$$

where α is a small positive constant of the order of 0.001. It is true that with this modification, it is unavoidable that during the gimbal transit, small torques could act on the spacecraft. Figure 12 shows the gimbal reorientation using the preceding scheme. The initial gimbal angles are σ = [0 deg, 0 deg, 0 deg, 0 deg]^T and the final gimbal angles are σ = [45 deg, − 45 deg,

45 deg, -45 deg]^T. The gimbal rates are shown in Fig. 13. It is evident that as the singularity is reached, the gimbal rates approach zero and it becomes necessary to to use the correction given by Eq. (18). Figure 14 shows the gain variation and it is clear that, for this example, the output torque on the spacecraft is negligible.

Conclusions

A new methodology for determining preferred initial gimbal-angle sets for SCMG clusters is presented. It is assumed that torque- and angular-momentum envelopes are known a priori. These need not be known exactly but in a qualitative sense. The basic element of this procedure is back integration of the CMG torque equation from the final conditions to the initial conditions. The procedure can be applied to any number of CMGs (more than three) in a cluster. Several examples, including active momentum management and attitude control of the space station, are presented. It is shown that singularity avoidance for a variety of problems can be easily achieved by selecting proper initial gimbal angles. Except in one instance, the gimbal-angle set $\sigma = [45 \text{ deg} \quad -45 \text{ deg} \quad 45 \text{ deg} \quad -45 \text{ deg}]^T$ has been found to be applicable in all of the examples considered. Data regarding the preferred gimbal-angle sets for various torque and momentum conditions have to be stored on board to use this procedure in practice. A feedback scheme for positioning the gimbals is also discussed. If this is done slowly, the disturbance on the spacecraft is negligible and can be compensated for by a feedback control law. For this reason, the gimbal-reorientation control law has to be active along with the torque-producing control law.

It is true that there are many preferred sets for a given problem and one may be better than the others. To determine this, a meaningful performance index such as the integral sum squares of the gimbal rates can be utilized and an optimal control problem solved.

Acknowledgments

We thank Eric Ring and David Geller of NASA Johnson Space Center for many useful discussions. We are grateful for the support of the Texas Advanced Research and Technology Program (Project 4193-1987). Critical reviews by the reviewers are appreciated.

References

[1]Kennel, H. F., "Steering Law for Parallel-Mounted Double-Gimballed Control Moment Gyros," Rev. A, NASA TM-82390, Jan. 1981.

[2]Kennel, H. F., "A Control Law for Double-Gimballed Control Moment Gyros Used for Space Vehicle Attitude Control," NASA TM-64536, Aug. 1970.

[3]Margulies, G., and Aubrun, J. N., "Geometric Theory of Single Gimbal-Control Moment Gyro Systems," *Journal of Astronautical Sciences,* Vol. 26, No. 2, 1978, pp. 159–191.

[4]Yoshikawa, T., "Steering Law for Roof-Type Configuration Control Moment Gyro System," *Automatica* , Vol. 13, No. 4, 1977, pp. 359-368.

[5]Cornick, D. E., "Singularity-Avoidance Control Laws for Single Gimbal Control Moment Gyros," AIAA Paper 79-1698, Aug. 1979.

[6]Hefner, R. D., and McKenzie, C. H., "A Technique for Maximizing the Torque Capability of Control Moment Gyro Systems," American Astronautical Society, Paper 83-387, AAS Astrodynamics Conf., Lake Placid, NY, Aug. 1983.

[7]Bauer, S. R., "Single-Gimbal CMG Steering Laws," Charles Stark Draper, Inc., Cambridge, MA, Space Guidance and Navigation Memo 10E-87-06, May 1987.

[8]Meefe, M., "Control Moment Gyroscope Configurations for the Space Station," American Astronautical Society, Paper 88-040, 11th AAS Guidance and Control Conf., Keystone, CO, Feb. 1988.

[9] Blondin, J., et. al., "Design, Fabrication, and Test of a Prototype Double-Gimbal Control Moment Gyroscope for the NASA Space Station," American Astronautical Society, Paper 89-006, 12th Annual AAS Guidance and Control Conf., Keystone, CO, Feb. 1989.

[10]Wie, B., Byun, K., Warren, W. Geller, D., Long, D., and Sunkel, J., "A New Momentum Management Controller from the Space Station," AIAA Paper 88-4132, Aug. 1988.

[11]Warren, W., Wie, B., and Geller, D.,"Periodic-Disturbance Accomodating Control of the Space Station for Asymptotic Momentum Management," AIAA Paper 89-3476, Aug. 1989.

[12]Kurokawa, H., Yajima, N., and Usui, S., "A New Steering Law of a Single-Gimbal CMG System of Pyramid Configuration," *Proceedings of the 10th IFAC Symposium on Automatic Control in Space*, Pergamon, Oxford, England, UK, June 25–28, 1985, p. 249.

[13]Bedrossian, N. S., "Steering-Law Design for Redundant Single-Gimbal Control Moment Gyro Systems," M.S. Thesis, Mechanical Engineering, Massachusetts Inst. of Technology, Cambridge, MA, Aug. 1987.

[14]Geller, D., private communication, 1988.

[15]Nakamura, Y., and Hanafusa, H., "Inverse Kinematic Solutions with Singularity Robustness for Robot Manipulator Control," *Journal of Dynamic Systems, Measurement, and Control* , Vol. 108, Sept. 1986, pp. 163-171.